DYNAMIC SINGULARITIES
IN FREE-FLOATING SPACE MANIPULATORS

Evangelos Papadopoulos, Member ASME
Department of Mechanical Engineering &
McGill Research Centre for Intelligent Machines
McGill University
Montreal, PQ H3A 2A7, Canada

Steven Dubowsky, Fellow ASME
Department of Mechanical Engineering
Massachusetts Institute of Technology
77 Massachusetts Avenue,
Cambridge, MA 02139

ABSTRACT

Dynamic Singularities are shown for free-floating space manipulator systems where the spacecraft moves in response to manipulator motions without compensation from its attitude control system. At a dynamic singularity the manipulator is unable to move its end-effector in some inertial direction; thus dynamic singularities must be considered in the design, planning, and control of free-floating space manipulator systems. The existence and location of dynamic singularities cannot be predicted solely from the manipulator kinematic structure because they are functions of the dynamic properties of the system, unlike the singularities for fixed-base manipulators. Also analyzed are the implications of dynamic singularities to the nature of the system's workspace.

I.   INTRODUCTION

Robotic manipulators will play important roles in future space missions. The control of such space manipulators poses planning and control problems not found in terrestrial fixed-base manipulators due to the dynamic coupling between space manipulators and their spacecraft. A number of control techniques for such systems have been proposed; these schemes can be classified in three categories. In the first category, spacecraft position and attitude are controlled by reaction jets to compensate for any manipulator dynamic forces exerted on the spacecraft. In this case, control laws for earth-bound manipulators can be used, but the utility of such systems may be limited because manipulator motions can both saturate the reaction jet system and consume relatively large amounts of attitude control fuel, limiting the useful life of the system [1]. In the second category, the spacecraft attitude is controlled, although not its translation, by using reaction wheels or attitude control jets [2,4]. The control of these systems is somewhat more complicated than that of the first category, although a technique called the Virtual Manipulator (VM) can be used to simplify the problem [4-7]. The third proposed category assumes a free-floating system in order to conserve fuel or electrical power [4,6-11]. Such a system permits the spacecraft to move freely in response

to manipulator motions. Since the spacecraft's attitude control system does not operate during this mode of space manipulation, this mode becomes feasible when no external forces and torques act on the system, and when its total momentum is negligible. In practice, momentum dump maneuvers would be employed to remove any momentum that may accumulate [15]. Past work on the control of free-floating systems generally has proposed particular algorithms for free-floating systems and attempted to show their validity on a case by case basis [8-11]. However, algorithms which do not take into full account the system kinematics or dynamics have occasional problems [10,11]. This paper shows that these problems may be attributed to *dynamic singularities* which are not found in earth bound manipulators. These dynamic singularities must be considered in the design, planning, and control of these systems because of their important effects on the performance of free-floating space manipulators.

The existence of dynamic singularities is shown first by writing the kinematics and conservation equations in a compact, explicit form through the use of barycenters [12,13]. Then it is shown that the end-effector inertial linear and angular velocities can be expressed solely as a function of the velocities of the manipulator controlled joint angles, and that they do not depend upon the uncontrolled linear and angular velocity of the spacecraft. Next a Jacobian matrix, $\mathbf{J}^*$, is derived which relates the end-effector's linear and angular velocity in inertial space to the joint angular velocities. The rank of this Jacobian matrix is demonstrably deficient at given points in the manipulator's joint space which results in the manipulator being unable to move its end-effector in some direction in inertial space. These singular points cannot be determined solely from the kinematic structure of the system and instead depend upon a system's masses and inertias; hence they are called dynamic singularities. Dynamic singularities are *path dependent* because generally they are not fixed in a manipulator's inertial workspace. This is because the end-effector location in inertial space depends upon the *history* of the spacecraft attitude which is determined by the path taken by the end-effector. Finally, some regions in the inertial workspace exist, called the *Path Independent Workspace (PIW)*, where dynamic singularities will not exist for any path taken within this region, as opposed to other parts of the workspace, called the *Path Dependent Workspace*

(PDW), where the occurrence of dynamic singularities depends upon the path taken by the manipulator's end-effector.

II. JACOBIAN CONSTRUCTION FOR FREE-FLOATING MANIPULATORS

End-effector position and orientation can be obtained directly for a manipulator on a fixed-base or on a controlled vehicle as a function of a system's independent coordinates, namely of the manipulator joint angles and base position and attitude. However, end-effector position and orientation cannot be obtained directly in free-floating space manipulator systems because spacecraft position and attitude are coordinates which depend upon the history of a manipulator's motion. Still, provided that the system is initially at rest and that no external forces or torques act on it, a Jacobian $\mathbf{J}^*$ can be written for the system and provide a linear relationship between the controlled manipulator's joint angular rates $\dot{\mathbf{q}}$ and the end-effector linear and angular inertial velocities, $\dot{\mathbf{r}}_E, \boldsymbol{\omega}_E$ such that:

$$[\dot{\mathbf{r}}_E, \boldsymbol{\omega}_E]^T = \mathbf{J}^* \dot{\mathbf{q}} \tag{1}$$

Dynamic singularities arise when $\mathbf{J}^*$ becomes deficient. This Jacobian plays a similar role to Jacobians used by many fixed-base manipulator control algorithms which are functions of manipulator kinematics only. For example, Umetani and Yoshida proposed a resolved rate controller based on $\mathbf{J}^*$, called a Generalized Jacobian [9]. However, the construction of $\mathbf{J}^*$ depends on a system's dynamics.

Here, the kinematic and dynamic relationships are formulated for the free-floating manipulator system depicted in Figure 1 and used to find an expression for $\mathbf{J}^*$, based on the use of the barycenters [12,13]. This approach has similarities to the VM method since in both cases the kinematic equations are written with respect to the system's CM. The advantage of the method presented in this paper is that it yields a set of body-fixed vectors, called barycentric, which are sufficient to describe both the kinematics and the dynamics of free-floating systems. Each barycentric vector is fixed on one of the N+1 bodies of the system, moving with it, and has a

constant length which can be computed once. These two properties simplify the kinematic and dynamic modeling of free-floating systems. Both the Jacobian and the inertia matrix of a free-floating system can be expressed compactly and explicitly in terms of the barycentric vectors, [15].

The body 0 in Figure 1 represents the spacecraft and the bodies k (k=1,...,N) represent the N manipulator links. Manipulator joint angles and velocities are represented by the N×1 column vectors $\mathbf{q}$ and $\dot{\mathbf{q}}$. The spacecraft can translate and rotate in response to manipulator motions. Finally, the manipulator is assumed to have revolute joints and an open-chain kinematic configuration so that a system with an N Degree-of-Freedom (DOF) manipulator will have 6+N DOF.

To derive $\mathbf{J}^*$, we must write $\underline{\dot{\mathbf{r}}}_E$ and $\underline{\boldsymbol{\omega}}_E$ as functions of the links and spacecraft inertial angular velocities $\underline{\boldsymbol{\omega}}_i$ (i=0,...,N) and ultimately of the joint rates $\dot{\mathbf{q}}$. From Figure 1, it can be seen that the vector from the inertially fixed origin O to k body's center of mass (*CM*), $\underline{\mathbf{R}}_k$, is given by:

$$\underline{\mathbf{R}}_k = \underline{\mathbf{r}}_{cm} + \underline{\boldsymbol{\rho}}_k \qquad\qquad k = 0,...,N \qquad\qquad (2)$$

where $\underline{\mathbf{r}}_{cm}$ and $\underline{\boldsymbol{\rho}}_k$ are defined in Figure 1. The end-point position vector, $\underline{\mathbf{r}}_E$, can be derived from $\underline{\mathbf{R}}_N$ as:

$$\underline{\mathbf{r}}_E = \underline{\mathbf{r}}_{cm} + \underline{\boldsymbol{\rho}}_N + \underline{\mathbf{r}}_N \qquad\qquad\qquad (3)$$

The $\underline{\boldsymbol{\rho}}_k$ vectors are defined uniquely by the free-floating system configuration and, thus, they can be expressed as sums of the weighted, body-fixed vectors $\underline{\mathbf{l}}_i$, and $\underline{\mathbf{r}}_i$ (i=0,...,N), defined in Figure 1. Indeed, from Figure 1 we have the following N equations in N+1 unknowns:

$$\underline{\boldsymbol{\rho}}_k - \underline{\boldsymbol{\rho}}_{k-1} = \underline{\mathbf{r}}_{k-1} - \underline{\mathbf{l}}_k \qquad\qquad k = 1,...,N \qquad\qquad (4)$$

Since the $\underline{\boldsymbol{\rho}}_k$ vectors are defined with respect to the system *CM*, it holds that:

$$\sum_{k=0}^{N} m_k \underline{\boldsymbol{\rho}}_k = 0 \qquad\qquad\qquad (5)$$

where m_k is the mass of body k. Equations (4) and (5) can be solved for $\underline{\boldsymbol{\rho}}_k$ as a function of $\underline{\mathbf{r}}_k$ and $\underline{\mathbf{l}}_k$, yielding:

$$\underline{\rho}_k = \sum_{i=1}^{k} (\underline{r}_{i-1} - \underline{l}_i)\, \mu_i - \sum_{i=k+1}^{N} (\underline{r}_{i-1} - \underline{l}_i)(1-\mu_i) \qquad\qquad k = 0,...,N \qquad\qquad (6)$$

where μ_i represents the mass distribution defined by:

$$\mu_i \equiv \begin{cases} 0 & i = 0 \\ \displaystyle\sum_{j=0}^{i-1} \frac{m_j}{M} & i = 1...N \\ 1 & i = N+1 \end{cases} \qquad\qquad (7)$$

M is the total system mass. Equation (6) can be simplified using the notion of a barycenter (*BC*) [12,13]. The barycenter location for the ith body with respect its *CM* is defined by the body fixed vector $\underline{c}_i$ shown in Figure 2 and given by:

$$\underline{c}_i = \underline{l}_i\, \mu_i + \underline{r}_i\, (1-\mu_{i+1}) \qquad\qquad i = 0,...,N \qquad\qquad (8)$$

The barycenter of the ith body can be found equivalently by adding a point mass equal to $M\mu_i$ to joint i, and a point mass equal to $M(1-\mu_{i+1})$ to joint i+1, forming an *augmented body* [12,13]. The barycenter is then the center of mass of the augmented body as shown in Figure 2. Figure 2 also shows a set of *body-fixed* vectors which are defined by:

$$\underline{c}_i^{*} = -\,\underline{c}_i \qquad\qquad (9a)$$

$$\underline{r}_i^{*} = \underline{r}_i - \underline{c}_i \qquad\qquad (9b)$$

$$\underline{l}_i^{*} = \underline{l}_i - \underline{c}_i \qquad\qquad (9c)$$

Using Equations (9), Equation (8) can be rewritten as:

$$M\,\mu_i\,\underline{l}_i^{*} + M\,(1-\mu_{i+1})\,\underline{r}_i^{*} + m_i\,\underline{c}_i^{*} = 0 \qquad\qquad (10)$$

It can be shown then that Equation (6) can be written in a compact and general form as:

$$\underline{\boldsymbol{\rho}}_k \ = \ \sum_{i=0}^{N} \underline{\mathbf{v}}_{ik} \qquad\qquad k = 0,...,N \qquad\qquad (11)$$

where the barycentric vectors $\underline{\mathbf{v}}_{ik}$ are given by the following selection law, [15]:

$$\underline{\mathbf{v}}_{ik} \equiv \begin{Bmatrix} \underline{\mathbf{r}}_i^* & i<k \\ \underline{\mathbf{c}}_i^* & i=k \\ \underline{\mathbf{l}}_i^* & i>k \end{Bmatrix} \qquad\qquad (12)$$

Equation (11) reveals an interesting characteristic of space manipulators, namely that the position of the center of mass of link k in inertial space depends on the position of *all* links, including the ones *after* link k as well as on the position of the base. This is to be contrasted with the case of earth-bound manipulators where the position of a link depends on the positions of the *previous* links only.

Since each $\underline{\mathbf{v}}_{ik}$ is defined by vectors fixed in body i which rotates with angular velocity $\underline{\boldsymbol{\omega}}_i$, and because we assume that the manipulator has no prismatic joints, the time derivative of $\underline{\boldsymbol{\rho}}_k$ is simply given by:

$$\dot{\underline{\boldsymbol{\rho}}}_k \ = \ \sum_{i=0}^{N} \underline{\boldsymbol{\omega}}_i \times \underline{\mathbf{v}}_{ik} \qquad\qquad k = 0,...,N \qquad\qquad (13)$$

Differentiating Equations (3) and combining the results with Equation (13) yields the following expression for the end-effector inertial velocity $\dot{\underline{\mathbf{r}}}_E$:

$$\dot{\underline{\mathbf{r}}}_E \ = \ \dot{\underline{\mathbf{r}}}_{cm} + \sum_{i=0}^{N} \underline{\boldsymbol{\omega}}_i \times \underline{\mathbf{v}}_{iN} + \underline{\boldsymbol{\omega}}_N \times \underline{\mathbf{r}}_N \qquad\qquad (14)$$

For this system the linear momentum vector with respect to the origin **O** is:

$$\underline{\mathbf{p}} \ = \ M\dot{\underline{\mathbf{r}}}_{cm} = \ \sum_{k=0}^{N} m_k \dot{\underline{\mathbf{R}}}_k \qquad\qquad (15)$$

In the absence of external forces, and assuming zero initial *CM* velocity, $\mathbf{p}$ is zero. Then $\dot{\underline{\mathbf{r}}}_{cm}$ is zero and $\underline{\mathbf{r}}_{cm}$ is constant. We can assume that $\underline{\mathbf{r}}_{cm}$ is zero without loss of generality, which is equivalent to choosing the inertial origin, **O**, to be at the *CM*. Consequently:

$$\dot{\underline{\mathbf{r}}}_E = \sum_{i=0}^{N} \underline{\boldsymbol{\omega}}_i \times \underline{\mathbf{v}}_{iN} + \underline{\boldsymbol{\omega}}_N \times \underline{\mathbf{r}}_N \equiv \sum_{i=0}^{N} \underline{\boldsymbol{\omega}}_i \times \underline{\mathbf{v}}_{iN}' \tag{16}$$

where $\underline{\mathbf{v}}_{iN}'$ is equal to $\underline{\mathbf{v}}_{iN}$ for all i,k except for $\underline{\mathbf{v}}_{NN}'$, for which it is given by $\underline{\mathbf{v}}_{NN}' = \underline{\mathbf{v}}_{NN} + \underline{\mathbf{r}}_N$.

The end-effector inertial angular velocity required to find $\mathbf{J}^*$, see Equation (1), is the inertial velocity of the last body in the chain given by:

$$\underline{\boldsymbol{\omega}}_E = \underline{\boldsymbol{\omega}}_N \tag{17}$$

The inertial angular velocity $\underline{\boldsymbol{\omega}}_j$ of the jth body can be written as a function of the relative angular velocity of body i with respect to body i-1 (the joint velocity of joint i), called $\underline{\boldsymbol{\omega}}_i^{i-1}$, as:

$$\underline{\boldsymbol{\omega}}_j = \underline{\boldsymbol{\omega}}_0 + \sum_{i=1}^{j} \underline{\boldsymbol{\omega}}_i^{i-1} \qquad j = 1,...,N \tag{18}$$

Equations (16), (17) and (18) relate the end-effector linear and angular velocities in inertial coordinates $\dot{\underline{\mathbf{r}}}_E$ and $\underline{\boldsymbol{\omega}}_E$ to the controlled relative angular velocities $\underline{\boldsymbol{\omega}}_i^{i-1}$ and to the spacecraft inertial angular velocity, $\underline{\boldsymbol{\omega}}_0$. Although $\underline{\boldsymbol{\omega}}_0$ is uncontrolled, it can be found as a function of the controlled joint rates by using the principle of the angular momentum conservation. The system angular momentum vector with respect to the inertial origin is given by:

$$\underline{\mathbf{h}} = \underline{\mathbf{r}}_{cm} \times \underline{\mathbf{p}} + \sum_{k=0}^{N} \{ \underline{\mathbf{I}}_k \cdot \underline{\boldsymbol{\omega}}_k + m_k \underline{\boldsymbol{\rho}}_k \times \dot{\underline{\boldsymbol{\rho}}}_k \} \tag{19}$$

where $\underline{\mathbf{I}}_k$ is the inertia dyadic of body k with respect to its center of mass. Since we assumed an initial zero linear momentum vector $\underline{\mathbf{p}}$, the first term in the right side of Equation (19) is identically equal to zero and the angular momentum with respect to **O** is equal to the angular momentum with

respect to the system *CM*, $\underline{\mathbf{h}}_{cm}$. Using Equations (11) and (13), Equation (19) can be written as, [15]:

$$\underline{\mathbf{h}} = \underline{\mathbf{h}}_{cm} = \sum_{j=0}^{N} \sum_{i=0}^{N} \sum_{k=0}^{N} \underline{\mathbf{D}}_{ijk} \bullet \underline{\boldsymbol{\omega}}_j \tag{20}$$

where:

$$\underline{\mathbf{D}}_{ijk} = \underline{\mathbf{I}}_i \, \delta_{ij}\delta_{jk} + m_k \left\{ (\underline{\mathbf{v}}_{ik} \bullet \underline{\mathbf{v}}_{jk}) \underline{\mathbf{1}} - \underline{\mathbf{v}}_{jk}\underline{\mathbf{v}}_{ik} \right\} \qquad i, j, k = 0,...,N$$
$$\tag{21}$$

The dyadics $\underline{\mathbf{D}}_{ijk}$ are functions of the distribution of inertia through the system and are formed from the barycentric vectors $\underline{\mathbf{v}}_{ik}$. The terms δ_{ij}, δ_{jk} are Kronecker deltas.

It can be shown that the angular momentum given by Equation (20) can be written as [15]:

$$\underline{\mathbf{h}}_{cm} = \sum_{j=0}^{N} \sum_{i=0}^{N} \underline{\mathbf{D}}_{ij} \bullet \underline{\boldsymbol{\omega}}_j \tag{22}$$

with $\underline{\mathbf{D}}_{ij}$ derived from Equation (21) with the help of Equation (10) and given by:

$$\underline{\mathbf{D}}_{ij} \equiv \begin{cases} - M \left\{ (\underline{\mathbf{l}}_j^* \bullet \underline{\mathbf{r}}_i^*) \underline{\mathbf{1}} - \underline{\mathbf{l}}_j^* \, \underline{\mathbf{r}}_i^* \right\} & i<j \\[2mm] \underline{\mathbf{I}}_i + \sum_{k=0}^{N} m_k \left\{ (\underline{\mathbf{v}}_{ik} \bullet \underline{\mathbf{v}}_{ik}) \underline{\mathbf{1}} - \underline{\mathbf{v}}_{ik} \, \underline{\mathbf{v}}_{ik} \right\} & i=j \\[2mm] - M \left\{ (\underline{\mathbf{r}}_j^* \bullet \underline{\mathbf{l}}_i^*) \underline{\mathbf{1}} - \underline{\mathbf{r}}_j^* \, \underline{\mathbf{l}}_i^* \right\} & i>j \end{cases} \tag{23}$$

where $\underline{\mathbf{1}}$ is the unit dyadic [15]. In the absence of external torques, the system angular momentum is constant. We further assume that during free-floating operation, the system momentum is zero. If momentum accumulates, the system may be able to continue operating for a limited period of time, [15]. In practice, the spacecraft's attitude control system would be turned on and perform a momentum dump maneuver in order to eliminate any accumulated momentum [15]. Equation (22) cannot be further integrated (with the exception of N=1) and must be carried along. Equations (16), (17), (18) and (22) are sufficient to describe the motion of the end-effector in inertial space as a

function of a free-floating system's joint angular velocities, one in which the position and attitude of the spacecraft is not controlled.

The above vector formulation is independent of specific frames of reference. However, to construct the system Jacobian $\mathbf{J}^*$, Equations (16), (17), (18) and (22) must be expressed in matrix form. For this purpose we assume all manipulator joints revolute; a reference frame with axes parallel to each body's principal axes is attached to each center of mass. The body inertia matrix expressed in this frame is diagonal. Bold lower case symbols represent column vectors, bold upper case matrices. Right superscripts must be interpreted as "with respect to," left as "expressed in frame." A missing left superscript implies a column vector expressed in the inertial frame.

The column vectors $^i\mathbf{v}_{ik}$ expressed in frame i are transformed in the inertial frame as follows:

$$\mathbf{v}_{ik} = \mathbf{T}_i\,{}^i\mathbf{v}_{ik} = \mathbf{T}_0\,{}^0\mathbf{v}_{ik} \tag{24a}$$

$$^0\mathbf{v}_{ik} = {}^0\mathbf{T}_i\,{}^i\mathbf{v}_{ik} \tag{24b}$$

where $\mathbf{T}_i$ is a transformation matrix that is given by:

$$\mathbf{T}_i\,(\mathbf{e},\, n,\, q_1,...,\, q_i) = \mathbf{T}_0(\mathbf{e},\, n)\,{}^0\mathbf{T}_i\,(q_1,...,\, q_i) \tag{25a}$$

$$^0\mathbf{T}_i\,(q_1,...,\, q_i) = {}^0\mathbf{A}_1(q_1)...{}^{i-1}\mathbf{A}_i(q_i) \tag{25b}$$

Note that $^{i-1}\mathbf{A}_i(q_i)$ transforms a column vector expressed in frame i to a column vector in frame i-1 and is a function of the relative joint angle of the two frames, q_i. The inertia matrices $\mathbf{D}_{ij}$ can be expressed in the spacecraft frame according to the following equation:

$$^0\mathbf{D}_{ij} = \mathbf{T}_0{}^T\,\mathbf{D}_{ij}\,\mathbf{T}_0 \qquad\qquad i,\, j = 1,...,N \tag{26}$$

The 3×3 transformation matrix $\mathbf{T}_0$ can be computed using the Euler parameters $\mathbf{e}$ and n [16]:

$$\mathbf{T}_0(\mathbf{e},\, n) = (n^2 - \mathbf{e}^T\mathbf{e}\,)\,\mathbf{1} + 2\,\mathbf{e}\,\mathbf{e}^T + 2\,n\,\mathbf{e}^\times \tag{27}$$

$$\mathbf{e}\,(\mathbf{a},\, \theta) = \mathbf{a}\,\sin(\theta/2) \tag{28a}$$

$$n(\mathbf{a}, \theta) = \cos(\theta/2) \tag{28b}$$

where $\mathbf{a}$ is the unit vector of the instant axis about which the spacecraft is rotated for an angle θ, the ^{T} superscript denotes transposition, and the $^{\times}$ superscript denotes a skew-symmetric matrix that is formed from an $\mathbf{e}$ according to:

$$\mathbf{e}^{\times} = \begin{bmatrix} 0 & -e_z & e_y \\ e_z & 0 & -e_x \\ -e_y & e_x & 0 \end{bmatrix} \tag{29}$$

$\mathbf{1}$ is the 3×3 identity matrix.

The scalar form of Equation (19) can now be written as:

$$\boldsymbol{\omega}_j = \boldsymbol{\omega}_0 + \boldsymbol{\omega}_j^0 = \boldsymbol{\omega}_0 + \mathbf{T}_0 \sum_{i=1}^{j} {}^0\mathbf{T}_i \, {}^i\mathbf{u}_i \, \dot{q}_i \tag{30a}$$

$$= \boldsymbol{\omega}_0 + \mathbf{T}_0 \, {}^0\mathbf{F}_j \, \dot{\mathbf{q}} \qquad\qquad j = 1,...,N \tag{30b}$$

where $^i\mathbf{u}_i$ is the unit column vector in frame i parallel to the revolute axis through joint i, and $^0\mathbf{F}_j$ is a 3×N matrix given by:

$${}^0\mathbf{F}_j \equiv [\,{}^0\mathbf{T}_1 \, {}^1\mathbf{u}_1, \, {}^0\mathbf{T}_2 \, {}^2\mathbf{u}_2,..., \, {}^0\mathbf{T}_j \, {}^j\mathbf{u}_j, \, \mathbf{0}\,] \qquad j = 1,...,N \tag{31}$$

where $\mathbf{0}$ is a 3×(N-j) zero element matrix, and:

$$\mathbf{q} = [\,q_1, q_2,..., q_j,..., q_N\,]^{T} \tag{32}$$

Using Equations (25) through (32), Equations (16), (17) and (22) yield:

$$\dot{\mathbf{r}}_E = \mathbf{T}_0 \{\,{}^0\mathbf{J}_{11} \, {}^0\boldsymbol{\omega}_0 + {}^0\mathbf{J}_{12} \, \dot{\mathbf{q}}\,\} \tag{33a}$$

$$\boldsymbol{\omega}_E = \mathbf{T}_0 \{\,{}^0\boldsymbol{\omega}_0 + {}^0\mathbf{J}_{22} \, \dot{\mathbf{q}}\,\} \tag{33b}$$

$$\mathbf{0} = {}^0\mathbf{D} \, {}^0\boldsymbol{\omega}_0 + {}^0\mathbf{D}_q \, \dot{\mathbf{q}} \tag{33c}$$

where:

$$^0\mathbf{J}_{11} \equiv -\sum_{i=0}^{N} [^0\mathbf{T}_i\,^i\mathbf{v}_{iN}']^{\times} \qquad ^0\mathbf{J}_{12} \equiv -\sum_{i=1}^{N} [^0\mathbf{T}_i\,^i\mathbf{v}_{iN}']^{\times}\,^0\mathbf{F}_i \qquad ^0\mathbf{J}_{22} \equiv \,^0\mathbf{F}_N \qquad (34a)$$

$$^0\mathbf{D}_j \equiv \sum_{i=0}^{N} \,^0\mathbf{D}_{ij} \; (j=0,...,N) \qquad ^0\mathbf{D} \equiv \sum_{j=0}^{N} \,^0\mathbf{D}_j \qquad ^0\mathbf{D}_\mathbf{q} \equiv \sum_{j=1}^{N} \,^0\mathbf{D}_j\,^0\mathbf{F}_j \quad (34b)$$

The term $^0\mathbf{D}_{ij}$ (i,j=0,...,N) represents inertia matrices, derived according to Equation (23); these are expressed in the spacecraft frame. Equations (33a) and (34b) reflect the fact that the motion of the end-effector is the vector sum of two partial velocities. The first is due to the motion of the joints, the second to the resulting motion of the spacecraft caused by dynamic coupling. Equation (33c) expresses the conservation of angular momentum. $^0\mathbf{J}_{11}$ is a skew-symmetric 3×3 matrix whose elements correspond to the vector from the system *CM* to the end-effector, expressed in the spacecraft frame. $^0\mathbf{J}_{12}$ is a 3×N matrix whose N columns are the components of vectors starting at the manipulator joints and ending at the end-effector. Along with $^0\mathbf{J}_{22}$, they correspond to the Jacobian of the end-effector Virtual Manipulator, with the first link fixed. (This is equivalent to a fixed attitude spacecraft). $^0\mathbf{D}$ is the 3×3 inertia matrix of the whole system expressed in the space-craft frame at the system *CM* , while $^0\mathbf{D}_\mathbf{q}$ is a 3×N matrix and corresponds to the inertia of the system's moving parts. All the matrices in Equations (34a-b) depend on the system configuration **q**, only.

Equation (33c) can be used to eliminate the spacecraft angular velocity $^0\boldsymbol{\omega}_0$ from Equations (33a-b), and hence to derive the free-floating system Jacobian $\mathbf{J}^*$, defined in Equation (1) as:

$$\mathbf{J}^*(\mathbf{e},\mathbf{n},\mathbf{q}) = \text{diag}(\mathbf{T}_0,\mathbf{T}_0) \begin{bmatrix} -^0\mathbf{J}_{11}\,^0\mathbf{D}^{-1}\,^0\mathbf{D}_\mathbf{q} + \,^0\mathbf{J}_{12} \\ -^0\mathbf{D}^{-1}\,^0\mathbf{D}_\mathbf{q} + \,^0\mathbf{J}_{22} \end{bmatrix} \qquad (35a)$$

$$= \text{diag}(\mathbf{T}_0,\mathbf{T}_0)\,^0\mathbf{J}^*(\mathbf{q}) \qquad (35b)$$

$$^0\mathbf{J}^*(\mathbf{q}) \equiv \begin{bmatrix} -^0\mathbf{J}_{11} \, ^0\mathbf{D}^{-1} \, ^0\mathbf{D}_\mathbf{q} + \, ^0\mathbf{J}_{12} \\ -^0\mathbf{D}^{-1} \, ^0\mathbf{D}_\mathbf{q} + \, ^0\mathbf{J}_{22} \end{bmatrix} \tag{35c}$$

Both $\mathbf{J}^*$ and $^0\mathbf{J}^*$ are 6×N matrices. Note that if N is equal to six, then $\mathbf{J}^*$ is square and, if not singular, can be inverted. Note also that diag($\mathbf{T}_0,\mathbf{T}_0$) is always non-singular, because $\mathbf{T}_0$ is always non-singular. If N is less than six, it is not possible to follow any given end-effector trajectory while, if N is greater than six, the manipulator is redundant and a generalized inverse technique can be used. We will assume in the rest of the paper that N is equal to six (no redundancy) unless it is otherwise noted. If $\mathbf{J}^*$ is going to be used for planning, $\mathbf{T}_0$ must be updated as the system moves. The new $\mathbf{e}$ and n are computed according to Equation (36) given below, see [16]:

$$\dot{\mathbf{e}} = 1/2 \, [\, \mathbf{e}^\times + n\,\mathbf{1} \,] \, ^0\boldsymbol{\omega}_0 \tag{36a}$$

$$\dot{n} = -1/2 \, \mathbf{e}^\mathrm{T} \, ^0\boldsymbol{\omega}_0 \tag{36b}$$

III.   DYNAMIC SINGULARITIES

Now we have shown a systematic and efficient way of constructing the Jacobian $\mathbf{J}^*$ that relates the motion of the end-effector as a function of the manipulator's controlled rates $\dot{\mathbf{q}}$ in spite of the uncontrolled motions of the spacecraft, and revealed the Jacobian's explicit structure. We will address the important question of when the Jacobian becomes singular. This is important for control and physical reasons, since nearly all planning algorithms as well as all resolved rate or acceleration control algorithms need to invert $\mathbf{J}^*$, given by Equation (35). Also the system Jacobian, for a manipulator position, must be invertible or of full rank in order *physically to move* the manipulator end-effector in all directions at that point in space.

Singularities occur for fixed-base non-redundant manipulators when end-effector velocity due to the motion of one joint is parallel to the velocity due to the motion of some other joint. At such points, at least one degree of freedom is lost and the rank of the manipulator Jacobian $\mathbf{J}$ is reduced, accordingly becoming singular. Singular points for fixed-base manipulators occur at workspace

boundaries or when there is alignment of joint axes. Given the kinematic structure of a manipulator, we can find all its singular configurations by solving the equation det[$\mathbf{J}$ ($\mathbf{q}$)]=0. The literature usually describes singular points in terms of fixed-base manipulator workspace positions instead of singular configurations or of singularities in the joint space because at any singular set of joint angles $\mathbf{q}_s$, there corresponds a singular point in the six DOF workspace. The obvious benefit is that the manipulator path planner or controller can be designed to avoid these workspace points. Singularities of fixed-base manipulators are *kinematic*, because it is sufficient to analyze the *kinematic structure* of the manipulator in order to identify them.

The singularities of $\mathbf{J}^*$ for a free-floating space system are obtained by examining Equation (35). First, it can be seen that the term diag($\mathbf{T}_0,\mathbf{T}_0$) is always square and invertible. Thus, any singular points of $\mathbf{J}^*$ are due to singular points of $^0\mathbf{J}^*(\mathbf{q})$ which can be found from the condition:

$$\det[^0\mathbf{J}^*(\mathbf{q})] \; = \; 0 \tag{37}$$

Equation (37) proves that all singularities are functions of the manipulator *configuration* with respect to its spacecraft, namely to the joint angles $\mathbf{q}$, not to the spacecraft attitude. These singularities correspond to singular points in the manipulator's *joint space*.

However, singular points in joint space cannot be mapped into unique points in the workspace. To show this, note first that due to Equations (3), (11), (24) and (25), the position $\mathbf{r}_E$, and orientation $\mathbf{T}_E$ of the manipulator's end-effector is a function of both the joint angles $\mathbf{q}$ and the spacecraft attitude $\mathbf{e}$,n:

$$\mathbf{r}_E \; = \; \boldsymbol{\rho}_N + \mathbf{r}_N = \; \mathbf{T}_0(\mathbf{e},n) \sum_{i=0}^{N} {}^0\mathbf{T}_i \, (q_1,..., q_i) \, {}^i\mathbf{v}_{iN}{}' \tag{38a}$$

$$\mathbf{T}_E \, (\mathbf{e}, n, q_1,..., q_N) \; = \; \mathbf{T}_0(\mathbf{e}, n) \, {}^0\mathbf{T}_N \, (q_1,..., q_N) \tag{38b}$$

If we are given the location and orientation of the end-effector, Equations (38) cannot be inverted to yield the manipulator's angles, even when N=6, unlike in fixed-based manipulators. The reason for this is that the spacecraft attitude is not a function of the joint angles; it is a function of

the path of the manipulator in inertial or joint space, [8,11,15]. This path dependence is due to the non-integrability of the angular momentum of the system, as given by Equation (33c), see also [11,15]. A result of this property is that if the end-effector returns to its initial inertial location and orientation after having followed a closed path in inertial space, the spacecraft's orientation and the manipulator's configuration will be different than the initial ones, [6,11]. Hence, each point in the manipulator workspace can be reached with infinite system configurations $\mathbf{q}$ and spacecraft attitudes ($\mathbf{e}$,n). Therefore, an end-effector location in the workspace can be singular or not depending on whether the manipulator reaches this location in a singular configuration $\mathbf{q}$. Thus the free-floating manipulator singularities in the workspace are path *dependent*.

In addition, $^0\mathbf{J}^*(\mathbf{q})$ in Equation (35c) depends on both the kinematic and mass properties expressed by the submatrices $^0\mathbf{J}_{12}$ and $^0\mathbf{J}_{22}$, and on the inertia distribution of the manipulator and the spacecraft, see Equations (23) and (34). As noted earlier, all $^0\mathbf{D}_{ij}$ matrices are functions of the system configuration and, hence, this distribution is configuration dependent. As a result, any singular configurations cannot be predicted by examining the kinematic structure of the manipulator alone. Since the singularities of $\mathbf{J}^*$ depend on the system's dynamic parameters, its mass and inertia properties, we call them *dynamic singularities*.

The dynamic singularities of a free-floating manipulator space manipulator system can be explained physically by noting that the end-effector velocity $[\dot{\mathbf{r}}_E, \boldsymbol{\omega}_E]^T$, given by Equation (33), is the vectorial sum of a part that depends on the motion of the joints, expressed by $\dot{\mathbf{q}}$, and to a part which corresponds to the reaction of the spacecraft, expressed by the dependent angular velocity $^0\boldsymbol{\omega}_0$. The magnitude of this second part depends on the relative magnitude of the manipulator and spacecraft inertias as expressed by the matrices $^0\mathbf{D}_\mathbf{q}$ and $^0\mathbf{D}$, respectively, see Equation (33c). The larger $^0\mathbf{D}$ is, the smaller the effect of the dynamic coupling between the manipulator and its spacecraft is. As in the case of fixed-based systems, $\mathbf{J}^*$ becomes singular when the end-effector velocity $[\dot{\mathbf{r}}_E, \boldsymbol{\omega}_E]^T$ due to the motion of just one joint angle, is parallel to the end-effector velocity due to some other joint angle. However, due to the coupling between the manipulator and its spacecraft, the configuration at which this happens is different from the one that would be predicted from the

kinematic structure of the system alone. In addition, singular configurations depend on the relative size of the inertias of the system. If the mass and inertia of the vehicle becomes very large, approximating a fixed-base manipulator, then all the dynamic terms in Equation (35) vanish and $\mathbf{J}^*$ reduces to the fixed-base manipulator Jacobian, while the dynamic singularities reduce to the ordinary kinematic singularities.

The conclusion of this analysis is that if the spacecraft of a space manipulator system is not actively controlled but is free-floating, then dynamic singularities can occur. All resolved rate or resolved acceleration control schemes will fail because at these points, Equation (35) has no inverse. Control schemes that compute the desired joint torques by using a transposed Jacobian will fail to keep the desired end-effector velocity because dynamic singularities represent an inherent *physical* limitation. The manipulator will move with a velocity that is the projection of the desired velocity on the allowed direction: the result may be large end-effector errors.

IV.   A PLANAR EXAMPLE

Consider the simple planar free-floating space manipulator system shown in Figure 3. The system parameters are given in Table I. As shown in the Appendix, the system Jacobian is:

$$\mathbf{J}^*(\theta,\mathbf{q}) = \begin{bmatrix} \cos(\theta) & -\sin(\theta) \\ \sin(\theta) & \cos(\theta) \end{bmatrix} {}^0\mathbf{J}^*(\mathbf{q}) \tag{39a}$$

$${}^0\mathbf{J}^*(\mathbf{q}) = \frac{1}{D} \begin{bmatrix} -(\beta s_1 + \gamma s_{12})D_0 & \beta s_1 D_2 - \gamma s_{12}(D_0 + D_1) \\ -\alpha(D_1 + D_2) + (\beta c_1 + \gamma c_{12})D_0 & -(\alpha + \beta c_1)D_2 + \gamma c_{12}(D_0 + D_1) \end{bmatrix} \tag{39b}$$

where θ, q_1 and q_2, are defined in Figure 3, $s_1 = \sin(q_1)$, $c_{12} = \cos(q_1 + q_2)$ etc. The inertia scalar sums D, D_0, D_1 and D_2 are defined in the Appendix, see Equation (A13), and $\alpha \equiv {}^0r_0^* = 0.426$ m, $\beta \equiv {}^1r_1^* = 0.894$ m, and $\gamma \equiv {}^2c_2^* + r_2 = 0.968$ m. Since each D_i (i=0,1,2) and D are functions of $\mathbf{q}$, the Jacobian elements are more complicated functions of the $\mathbf{q}$ than their fixed-base counterparts. This Jacobian should be compared to the fixed-base manipulator Jacobian $\mathbf{J}$ which is given by:

$$\mathbf{J(q)} = \begin{bmatrix} -(l_1+r_1)s_1-(l_2+r_2)s_{12} & -(l_2+r_2)s_{12} \\ (l_1+r_1)c_1+(l_2+r_2)c_{12} & (l_2+r_2)c_{12} \end{bmatrix} \tag{40}$$

The same structure between $\mathbf{J}^*$ or $^0\mathbf{J}^*(\mathbf{q})$ and $\mathbf{J(q)}$ can be seen.

Table I. The system parameters.

Body	l_i (m)	r_i (m)	m_i (Kg)	I_i (Kg m^2)
0	.5	.5	40	6.667
1	.5	.5	4	0.333
2	.5	.5	3	0.250

In order to invert $\mathbf{J}^*$ given by Equation (38), the 2×2 matrix, $^0\mathbf{J}^*(\mathbf{q})$, must be inverted. First its determinant becomes zero when:

$$\alpha\beta D_2(q_1,q_2)\sin(q_1)+\beta\gamma D_0(q_1,q_2)\sin(q_2)-\alpha\gamma D_1(q_1,q_2)\sin(q_1+q_2) = 0 \tag{41}$$

The values of q_1 and q_2 which satisfy Equation (41) and result in dynamically singular configurations can be plotted in joint space as shown in Figure 4. This Figure also shows that conventional kinematic singularities like $q_1=k\pi$, $q_2=k\pi$, k=0,±1,... still satisfy Equation (41). However, infinitely more dynamically singular configurations exist which cannot be predicted from the kinematic structure of the manipulator.

Figure 3 shows the manipulator in the singular configuration at q_1=-65°, q_2=-11.41°: spacecraft attitude at θ=40°. This figure also shows the only available direction for the end-effector motion. The inertial motion of the end-effector in this configuration will be the shown, no matter how the joint actuators are driven. The best a control algorithm can do is to follow the available direction. *All* algorithms that use a Jacobian inverse, such as the resolved rate or resolved acceleration control algorithms, fail at such a point. Ones that use a pseudoinverse Jacobian or a Jacobian transpose will likely follow the available direction, but may result in large unrecoverable errors.

To demonstrate this problem, the manipulator end-point is commanded to reach the workspace point (1.5,1.5) starting from the initial location of (2,0) with initial attitude θ equal to 21° using a simple Transposed Jacobian Control algorithm, augmented by a velocity feedback term for increased stability margins [17]. This control algorithm assumes that the end-effector inertial position and velocity, $\mathbf{x}$ and $\dot{\mathbf{x}}$, can be calculated or measured directly. Assuming $\mathbf{x}$ and $\dot{\mathbf{x}}$ are measured, the control law is:

$$\boldsymbol{\tau} = \mathbf{J}^{*T} \{ \mathbf{K}_p (\mathbf{x}_{des} - \mathbf{x}) - \mathbf{K}_d \dot{\mathbf{x}} \} \quad (42)$$

where $\mathbf{x}_{des}$ is the inertial desired point location. The matrices $\mathbf{K}_p$ and $\mathbf{K}_d$ are diagonal. Note that this algorithm specifies the desired end-effector location; the path of the end-effector to this desired location is not specified in advance. If the control gains are large enough, then the motion of the end-point will be a straight line. The torque vector $\boldsymbol{\tau}$ is non-zero until the $(\mathbf{x}_{des} - \mathbf{x})$ and $\dot{\mathbf{x}}$ are zero or until the vector in the brackets in Equation (42) is in the null space of $\mathbf{J}^{*T}$.

Figure 5 shows the motion of the end-effector from the initial location at point A (2,0), towards the final location at point D (1.5,1.5). The control gain matrices are $\mathbf{K}_p = \text{diag}(5,5)$ and $\mathbf{K}_d = \text{diag}(15,15)$. Initially the end-effector path is initially almost a straight line. However, once the manipulator assumes a dynamically singular configuration at point B in Figure 5, the end-effector cannot move towards its desired position; rather it moves along the available direction converging finally to point C, for which $(\mathbf{x}_{des} - \mathbf{x})$ is in the null space of $\mathbf{J}^{*T}$. Any further motion beyond C is impossible. Figure 6 shows the time history of the spacecraft attitude and manipulator joint angles. The system reaches a dynamically singular configuration in about 5 seconds and thereafter oscillates about singular configurations until it finally converges to point C. Note again that an algorithm using a Jacobian inverse would fail at a location like point B.

Finally, it is interesting to note that when both m_0 and I_0 approach infinity, $\mathbf{J}^*$ approaches $\mathbf{J}$, the Jacobian derived for the same manipulator on a fixed-base, without any change in matrix size. To show this note that if the spacecraft is massive, $\beta \to l_1 + r_1$, $\gamma \to l_2 + r_2$, approaching the manipulator link lengths, $m_0/M \to 1$, $m_1/M \to 0$, $m_2/M \to 0$, $D_0/D \to 1$, $D_1/D \to 0$ and $D_2/D \to 0$. $\mathbf{T}_0$ becomes a

constant transformation from the manipulator base frame to the inertial frame, usually the unit matrix.

V. SPACE MANIPULATOR WORKSPACES

Space manipulators have more complex workspace characteristics than fixed-base manipulators, as shown by using the concept of the Virtual Manipulator. Vafa describes a *constrained* workspace, one where all points can be reached if the attitude of the spacecraft is controlled, but not its position [5]. This workspace is a sphere with its center at the system's *CM*. However, it can be shown that if the attitude is not controlled, as for a free-floating system, then points in this space can still always be reached by a suitable path selection [15]. For this reason we prefer to call this workspace the *reachable* workspace. What follows below shows that the nature of this workspace is related to a system's dynamic singularities.

We have proven already that a system's dynamic singularities are a unique function of the configuration and that their occurrence at a particular inertial workspace location is path dependent. Here we are interested in finding regions in the reachable workspace in which dynamic singularities will never occur.

Recall that dynamically singular configurations can be found from Equation (37). Its solution represents a family of hypersurfaces $\mathbf{Q}_{s,i}$ (i=1,2,...) in the manipulator *joint space*. These hypersurfaces are collections of points $\mathbf{q}_s$ that result in dynamically singular configurations. Further note that the transformation matrix $\mathbf{T}_0$ does not change the length of a vector; hence, the distance R of the end-effector location from the system *CM* can be written using Equation (38) as a function of the system's configuration $\mathbf{q}$ only:

$$R = R(\mathbf{q}) = \left\| \sum_{i=0}^{N} {}^{0}\mathbf{T}_i (q_1,..., q_i) \, {}^{i}\mathbf{v}_{iN}' \right\| \tag{43}$$

The symbol $\|\bullet\|$ denotes a vector's length. Equation (43) also defines a spherical shell in inertial space with its center at the *CM* and with a radius R. Hence, each singular configuration $\mathbf{q}_s$ is mapped according to Equation (43) to a spherical shell in inertial space. By the same token, each

hypersurface $\mathbf{Q}_{s,i}$ is mapped according to Equation (43) to a volume contained within the spherical shells with radii:

$$R_{min,i} = \min_{\mathbf{q}\_\mathbf{Q}_{s\,i}} R(\mathbf{q}) \qquad (i=1,2,...) \qquad (44a)$$

$$R_{max,i} = \max_{\mathbf{q}\_\mathbf{Q}_{s\,i}} R(\mathbf{q}) \qquad (i=1,2,...) \qquad (44b)$$

All workspace points that belong in this volume can be singular if they are reached in singular configurations $\mathbf{q}_s$. As shown earlier, this may happen or not depending on the path taken by the manipulator's end-effector. If there is more than one singular hypersurfaces, then there are more such volumes containing points that can lead to singular configurations. We call the union of all these volumes a *Path Dependent Workspace (PDW)*. The Path Dependent Workspace contains all reachable workspace locations that may be reached in singular configurations, depending upon the path taken by the end-effector. It follows that locations in the *PDW* can be reached with some paths but not with others; this justifies their name. In order to reach points belonging to the *PDW*, carefully selected paths must be employed.

Subtracting the *PDW* from the reachable workspace results in the *Path Independent Workspace (PIW)*. Due to its construction, this workspace region contains all reachable workspace locations that will *never* lead to dynamically singular configurations. It follows that all points in the Path Independent Workspace can be reached by any path, assuming that this path lies entirely in the *PIW*. It can be shown that the *PIW* is a subset of the *free workspace* defined by Vafa [15,5]. *PIW* or *PDW* spaces may reduce to zero depending on the case. A clear goal for the designer is to reduce the *PDW* and increase the *PIW*.

The construction of the *PIW* and *PDW* workspaces is demonstrated using the system illustrated in Figure 3. The distance R of the end-effector from the system *CM* given by Equation (43) is written as:

$$R = R(\mathbf{q}) = \sqrt{\alpha^2 + \beta^2 + \gamma^2 + 2\alpha\beta\cos(q_1) + 2\alpha\gamma\cos(q_1+q_2) + 2\beta\gamma\cos(q_2)} \qquad (45)$$

For this example, there are two hypersurfaces $\mathbf{Q}_s$ which are lines in the joint space (see Figure 4), and are found according to Equation (41). Each of these lines corresponds to pairs of q_1 and q_2, which are substituted in Equation (45). Then, the conditions in Equations (44a-b) result in two Path Dependent Workspaces, constrained by $(R_{min,1}, R_{max,1})$ and $(R_{min,2}, R_{max,2})$ respectively:

$$R_{min,1} = 0.352 \text{ m} = \alpha + \beta - \gamma \tag{46a}$$

$$R_{max,1} = 0.554 \text{ m} \tag{46b}$$

$$R_{min,2} = 1.436 \text{ m} \tag{47a}$$

$$R_{max,2} = 2.288 \text{ m} = \alpha + \beta + \gamma \tag{47b}$$

The *PIW* is then found by subtracting the two *PDW* regions defined above from the reachable workspace, see Figure 7. In general, the *PIW* is smaller than the free workspace defined in Reference [5]. When the end-effector path has points belonging to the *PDW*, such as path AB in Figure 7, the manipulator may assume a dynamically singular configuration because points in the *PDW* region can be dynamically singular, depending on the path. On the other hand, paths totally within the *PIW* region, such as path DE, can never lead to dynamically singular configurations.

To carry further the example of the previous paragraph, note that in the example, the commanded path was precisely path AB, shown in Figure 7. Since this path belongs in the *PDW*, a singularity occurred and point B, the final destination, could not be reached from the initial point A. However, the inability to reach point B from point A with a straight line path does not mean that point B is not reachable from point A. To show this, consider the path ACB, as shown in Figure 7. The end-effector is commanded to move to point C (1,0). It reaches this point with the following configuration $\theta = 39.6°$, $q_1 = -134.2°$, $q_2 = 134.4°$. Next, the end-effector is commanded to follow the square path around point C for approximately 9 times, clockwise. The side of this square is .4m. After this motion ends, the configuration of the system changes to $\theta = 73.63°$, $q_1 = -160.95°$, $q_2 = 117.34°$. The end-effector is next commanded to move to point B in a straight line and finally, it

arrives at point B, without any difficulty and with $\theta=21.29°$, $q_1=7.57°$, $q_2=41.90°$. It must be noted that this result is not sensitive at all to the number of rotations around C or to the location of C itself, as far as this is in the *PIW* so as to avoid dynamic singularities. The efficient construction of paths to reach points in the *PDW* is still an open area of research.

VI.   REDUCING THE EFFECT OF DYNAMIC SINGULARITIES

Maximizing the *PIW* clearly reduces the impact of dynamic singularities on a system's effectiveness. This can be achieved by recalling that dynamic singularities occur because the spacecraft is free to rotate as a result of manipulator motions, see Equation (33). If the spacecraft attitude is kept constant, $\boldsymbol{\omega}_0$ is zero, and the only singular points are due to the kinematic singularities; the *PIW* is maximum [15]. However, this method requires the active control of the spacecraft attitude which can increase system complexity and cost and reduce the system's useful life.

The *PIW* can also be maximized using manipulator redundancy. If the manipulator is at a singular configuration, the redundant degrees of freedom may be used to achieve the necessary end-effector velocity. This is an area which requires additional research.

If the spacecraft is made to be massive compared to the manipulator, $\mathbf{I}_0$ and $\mathbf{D}_0$ become large. For example, it can be seen from Equation (41) that if I_0 approaches infinity, the only singular configurations are the kinematic ones ($q_2 = \pm0°$, $\pm180°$). This means that if the inertia of the spacecraft is infinite, then no dynamic singularities occur and the *PIW* is equal to the maximum workspace. Although it is desirable in most cases to make the spacecraft as light as possible for a number of reasons, such as launch weight, a system's designer has the freedom to increase the system's inertia keeping its mass constant. Such a design would result in an increase in the system's *PIW*.

Finally, for the case where the manipulator acts in a plane, it can be shown that if the manipulator is mounted at the spacecraft's center of mass, the *PIW* is equal to the reachable workspace and the *PDW* is eliminated [14,15]. For the example discussed in Section IV, if ${}^0r_0^*$ or α are zero, the only singular configuration that exists is at q_2 equal to $k\pi$ (k=0,±1,...), see Equation

(41). This is a kinematic singularity and corresponds to the reachable workspace boundaries. If $^0r_0^*$ or α approach zero, then the two circles that define the *PIW*, shown in Figure 7, approach the reachable workspace boundaries, see Equations (46); hence the dynamic singularities become less important. In some cases it may be possible to use combinations of the various techniques discussed. For example, a system may be designed to have a large moment of inertia about one axis while the manipulator arm is mounted near the spacecraft *CM* in the other two dimensions.

V.   CONCLUSIONS

A general formulation describing the motion of a space manipulator system is presented. The system Jacobian is derived for a free-floating system where spacecraft position and attitude are not controlled. This Jacobian can be singular in configurations that are distinct from the usual kinematically singular configurations: a free-floating manipulator system exhibits singularities due to the dynamic coupling between link motions and the spacecraft. These singularities are called *dynamic singularities* and can be a serious problem for all planning and control algorithms that do not assume active control of spacecraft attitude. Consequently, their effects must be considered in the design of such systems.

Additionally, a workspace point may be singular or not depending on the end-effector path used to reach this point. Thus a manipulator's reachable workspace is divided in two regions. In the first, called a Path Independent Workspace, no dynamic singularities can occur; in the second, called a Path Dependent Workspace, dynamic singularities may occur depending on the path taken by the end-effector in the inertial space. Some notions are presented that may help in maximizing the Path Independent Workspace.

REFERENCES

[1] Dubowsky, S., Vance, E., and Torres, M., "The Control of Space Manipulators Subject to Spacecraft Attitude Control Saturation Limits," *Proc. of the NASA Conference on Space Telerobotics*, JPL, Pasadena, CA, Jan. 31-Feb. 2, 1989.

[2] Dubowsky, S., and Torres, M., "Path Planning for Space Manipulators to Minimize the Use of Attitude Control Fuel," *Proc. of the International Symposium on Artificial Intelligence, Robotics and Automation in Space (I-SAIRAS)*, Kobe, Japan, November 1990.

[3] Longman, R., Lindberg, R., and Zedd, M., "Satellite-Mounted Robot Manipulators-New Kinematics and Reaction Moment Compensation," *The International Journal of Robotics Research*, Vol. 6, No. 3, pp. 87-103, Fall 1987.

[4] Vafa, Z., and Dubowsky, S., "On the Dynamics of Manipulators in Space Using the Virtual Manipulator Approach," *Proc. of the IEEE International Conference on Robotics and Automation*, Raleigh, NC, March 1987.

[5] Dubowsky, S., and Vafa, Z., "A Virtual Manipulator for Space Robotic Systems," *Proc. of the Workshop on Space Telerobotics*, Pasadena, CA, January 1987.

[6] Vafa, Z., and Dubowsky, S., "On the Dynamics of Space Manipulators Using the Virtual Manipulator, with Applications to Path Planning," *The Journal of Astronautical Sciences*, Vol. 38, No. 4, October-December 1990, pp. 441-472.

[7] Vafa, Z., and Dubowsky, S., "The Kinematics and Dynamics of Space Manipulators: The Virtual Manipulator Approach," *The International Journal of Robotics Research*, Vol. 9, No. 4, August 1990, pp. 3-21.

[8] Alexander, H., and Cannon, R., "Experiments on the Control of a Satellite Manipulator," *Proc. of 1987 American Control Conference*, Seattle, WA, June 1987.

[9] Umetani, Y., and Yoshida, K., "Experimental Study on Two Dimensional Free-Flying Robot Satellite Model," *Proc. of the NASA Conference on Space Telerobotics*, Pasadena, CA, January 1989.

[10]   Masutani, Y., Miyazaki, F., and Arimoto, S., "Sensory Feedback Control for Space Manipulators," *Proc. of the IEEE International Conference on Robotics and Automation*, Scottsdale, AZ, May 1989.

[11]   Nakamura, Y., and Mukherjee, R., "Nonholonomic Path Planning of Space Robots," *Proc. of the IEEE International Conference on Robotics and Automation*, Scottsdale, AZ, May 1989.

[12]   Hooker, W., and Margulies, G., "The Dynamical Attitude Equations for an n-Body Satellite," *The Journal of Astronautical Sciences*, Vol XII, No 4, Winter 1965.

[13]   Wittenburg, J., *Dynamics of Rigid Bodies,* B.G. Teubner, Stuttgart, 1977.

[14]   Papadopoulos, E., and Dubowsky, D., "On the Dynamic Singularities in the Control of Free-Floating Space Manipulators," *Proceedings of the ASME Winter Annual Meeting*, San Fransisco, December 1989.

[15]   Papadopoulos, E., "On the Dynamics and Control of Space Manipulators," Ph.D. Thesis, Department of Mechanical Engineering, MIT, Cambridge, MA, October 1990.

[16]   Hughes, P., *Spacecraft Attitude Dynamics*, John Wiley, New York, NY, 1986.

[17]   Craig, J., *Introduction to Robotics, Mechanics and Control*, Addison Wesley, Reading, MA, 1986.

APPENDIX A

The planar two link system shown in Figure 3 assumes the two coordinates of the end-effector, x and y, are controlled by the two manipulator joint angles, q_1 and q_2. End-effector orientation is not controlled for this two DOF system (N=2), hence Equation (1) for this system is simply:

$$\dot{\mathbf{x}} = \dot{\mathbf{r}}_E = \frac{d}{dt} [x, y]^T = \mathbf{J}^* \dot{\mathbf{q}} \tag{A1}$$

with:

$$\mathbf{x} = \mathbf{r}_E = [x, y]^T \tag{A2}$$

$$\mathbf{q} = [q_1, q_2]^T \tag{A3}$$

while $\mathbf{J}^*$ given by Equation (35), becomes:

$$\mathbf{J}^*(\theta,\mathbf{q}) = \mathbf{T}_0(\theta)\ {}^0\mathbf{J}^*(\mathbf{q}) = \mathbf{T}_0 [-{}^0\mathbf{J}_{11}\ {}^0\mathbf{D}^{-1}\ {}^0\mathbf{D_q} + {}^0\mathbf{J}_{12}] \tag{A4}$$

where θ denotes the spacecraft attitude, as shown in Figure 3. For this example, the transformation matrix from the spacecraft frame to the inertial frame, $\mathbf{T}_0$, is given by:

$$\mathbf{T}_0(\theta) = Rot(\theta) = \begin{bmatrix} \cos(\theta) & -\sin(\theta) \\ \sin(\theta) & \cos(\theta) \end{bmatrix} \tag{A5}$$

Only the planar sub-part of the transformation matrices is used for simplicity. The transformation matrices ${}^0\mathbf{T}_i$ are found according to Equation (25):

$${}^0\mathbf{T}_1 = Rot(q_1)$$

$${}^0\mathbf{T}_2 = Rot(q_1)\ Rot(q_2) \tag{A6}$$

The following demonstrates the construction of the system inertia matrix. The matrices in Equation (A4) are assembled by first expressing all $\mathbf{v}_{ik}$ in Equation (12) in the frame of the ith body, according to Equations (7)-(9). For the sake of simplicity we assume that all $\mathbf{r}_i$ and $\mathbf{l}_i$ are

parallel to the x axis of the ith frame. Hence, only the x-component of the barycentric vectors ${}^i\mathbf{v}_{ik}$ is non-zero and given by:

$$
{}^0r_0^* = \frac{1}{M}\, r_0 m_0
$$

$$
{}^0c_0^* = -\frac{1}{M}\, r_0(m_1+m_2)
$$

$$
{}^0l_0^* = -\frac{1}{M}\, r_0(m_1+m_2) - l_0
$$

$$
{}^1r_1^* = \frac{1}{M}\, \left\{ r_1(m_0+m_1)+l_1 m_0 \right\}
$$

$$
{}^1c_1^* = \frac{1}{M}\, (l_1 m_0 - r_1 m_2)
$$

$$
{}^1l_1^* = -\frac{1}{M}\, \left\{ l_1(m_1+m_2)+r_1 m_2 \right\}
$$

$$
{}^2r_2^* = \frac{1}{M}\, l_2(m_0+m_1) + r_2
$$

$$
{}^2c_2^* = \frac{1}{M}\, l_2(m_0+m_1)
$$

$$
{}^2l_2^* = -\frac{1}{M}\, l_2 m_2 \tag{A7}
$$

where the total mass of the system, M, is given by:

$$
M = m_0 + m_1 + m_2 \tag{A8}
$$

For the planar case, the inertia matrices ${}^0\mathbf{D}_{ij}$ corresponding to Equation (3) reduce to the scalars ${}^0d_{ij}$ and are given by:

$$
{}^0d_{00} = I_0 + \frac{m_0(m_1+m_2)}{M}\, r_0{}^2
$$

$$
{}^0d_{10} = \frac{m_0 r_0}{M}\, \left\{ l_1(m_1+m_2) + r_1 m_2 \right\} \cos(q_1) = {}^0d_{01}
$$

$$^0d_{20} = \frac{m_0 m_2}{M} r_0 l_2 \cos(q_1 + q_2) = {}^0d_{02}$$

$$^0d_{11} = I_1 + \frac{m_0 m_1}{M} l_1{}^2 + \frac{m_1 m_2}{M} r_1{}^2 + \frac{m_0 m_2}{M}(l_1 + r_1)^2$$

$$^0d_{21} = \left\{ \frac{m_1 m_2}{M} r_1 l_2 + \frac{m_0 m_2}{M} l_2(l_1 + r_1) \right\} \cos(q_2) = {}^0d_{12}$$

$$^0d_{22} = I_2 + \frac{m_2(m_0 + m_1)}{M} l_2{}^2 \tag{A9}$$

Both ${}^i\mathbf{u}_i$ (i=1,2) vectors in Equation (17) are equal to $[0\ 0\ 1]^T$; the ${}^0\mathbf{F}_i$ matrices reduce to:

$$^0\mathbf{F}_1 = [1\quad 0]$$

$$^0\mathbf{F}_2 = [1\quad 1] \tag{A10}$$

For simplicity, set:

$$\alpha \equiv {}^0r_0^* \qquad\qquad \beta \equiv {}^1r_1^* \qquad\qquad \gamma \equiv {}^2c_2^* + r_2 \tag{A11}$$

Then the matrices in Equation (34) are given by:

$$^0\mathbf{J}_{11} = \begin{bmatrix} -\beta s_1 - \gamma s_{12} \\ \alpha + \beta c_1 + \gamma c_{12} \end{bmatrix}, \qquad ^0\mathbf{J}_{12} = \begin{bmatrix} -\beta s_1 - \gamma s_{12} & -\gamma s_{12} \\ \beta c_1 + \gamma c_{12} & \gamma c_{12} \end{bmatrix}, \quad ^0\mathbf{J}_{22} = {}^0\mathbf{F}_2 \tag{A12}$$

$$^0\mathbf{D}_j \equiv D_j = \sum_{i=0}^{2} {}^0d_{ij} \ (j=0,1,2), \qquad ^0\mathbf{D} \equiv D = D_0 + D_1 + D_2, \qquad ^0\mathbf{D}_q = [D_1 + D_2 \quad D_2] \tag{A13}$$

where $s_1 \equiv \sin(q_1)$, $c_{12} \equiv \cos(q_1 + q_2)$ etc. Finally, the system Jacobian $\mathbf{J}^*$ is assembled from Equations (A4) and (A7)-(A13) and given as Equation (38).
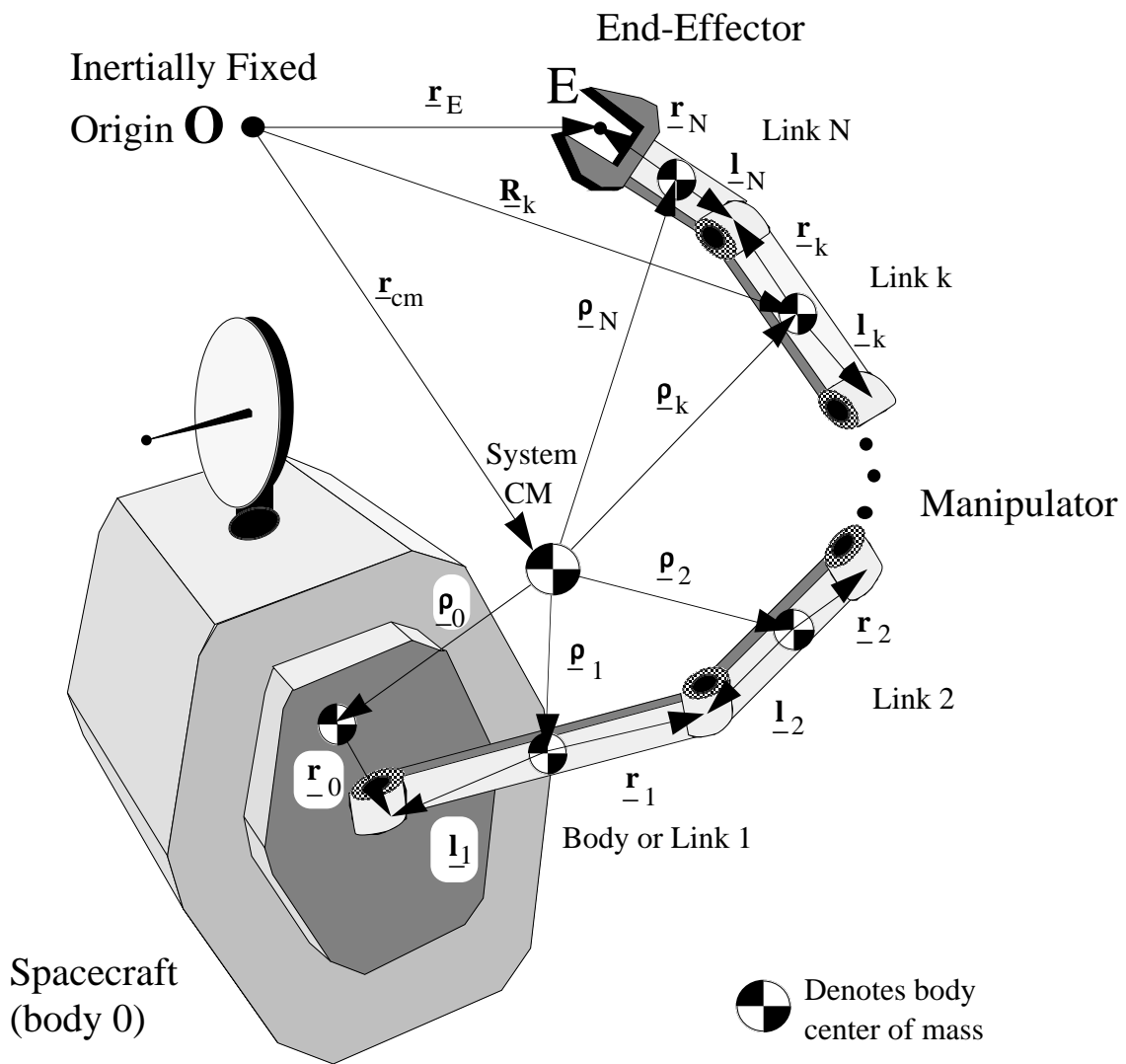
End-Effector

Inertially Fixed

Origin O

$\underline{r}_E$

E

$\underline{r}_N$

Link N

$\underline{R}_k$

$\underline{l}_N$

$\underline{r}_{cm}$

$\underline{r}_k$

Link k

$\underline{\rho}_N$

$\underline{l}_k$

$\underline{\rho}_k$

System
CM

Manipulator

$\underline{\rho}_0$

$\underline{\rho}_2$

$\underline{r}_2$

$\underline{\rho}_1$

Link 2

$\underline{l}_2$

$\underline{r}_0$

$\underline{r}_1$

$\underline{l}_1$

Body or Link 1

Spacecraft
(body 0)

Denotes body
center of mass

Figure 1. A free-floating space manipulator system.
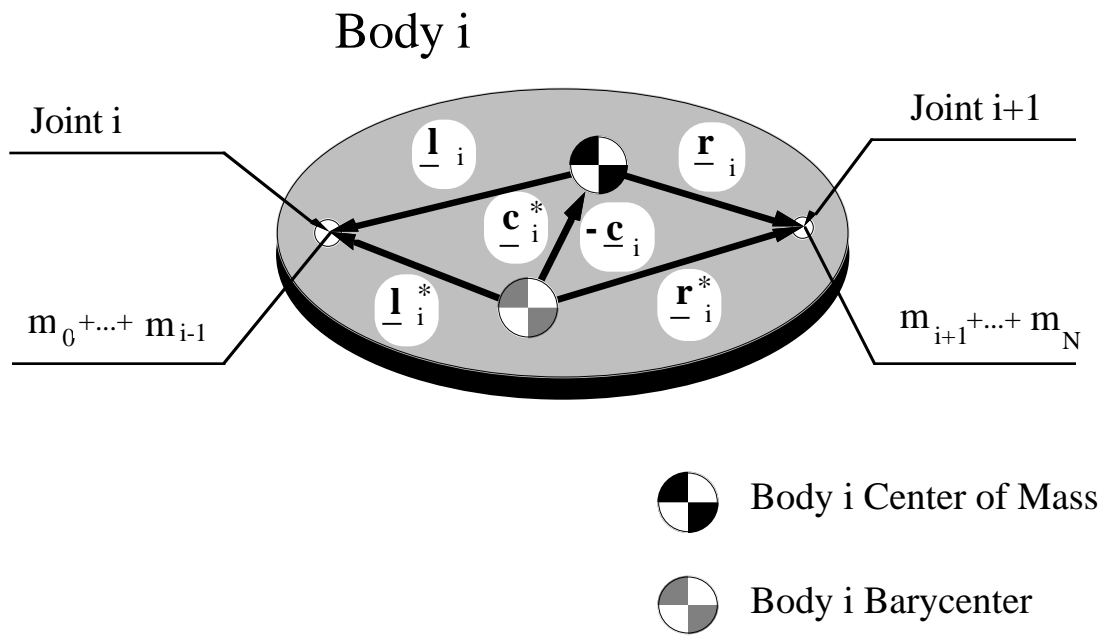
Figure 2. Definition of barycenters and vectors $\underline{\mathbf{r}}_i^*$, $\underline{\mathbf{l}}_i^*$, $\underline{\mathbf{c}}_i^*$.
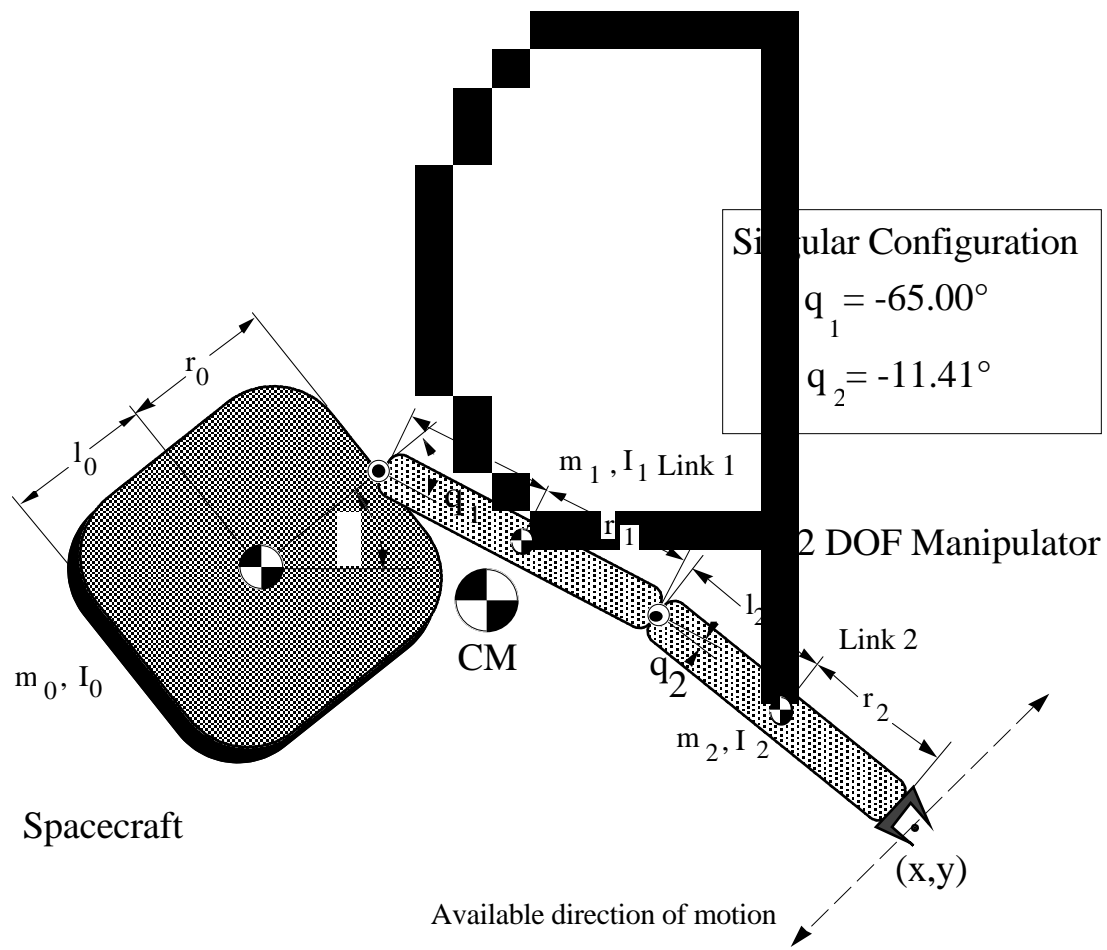
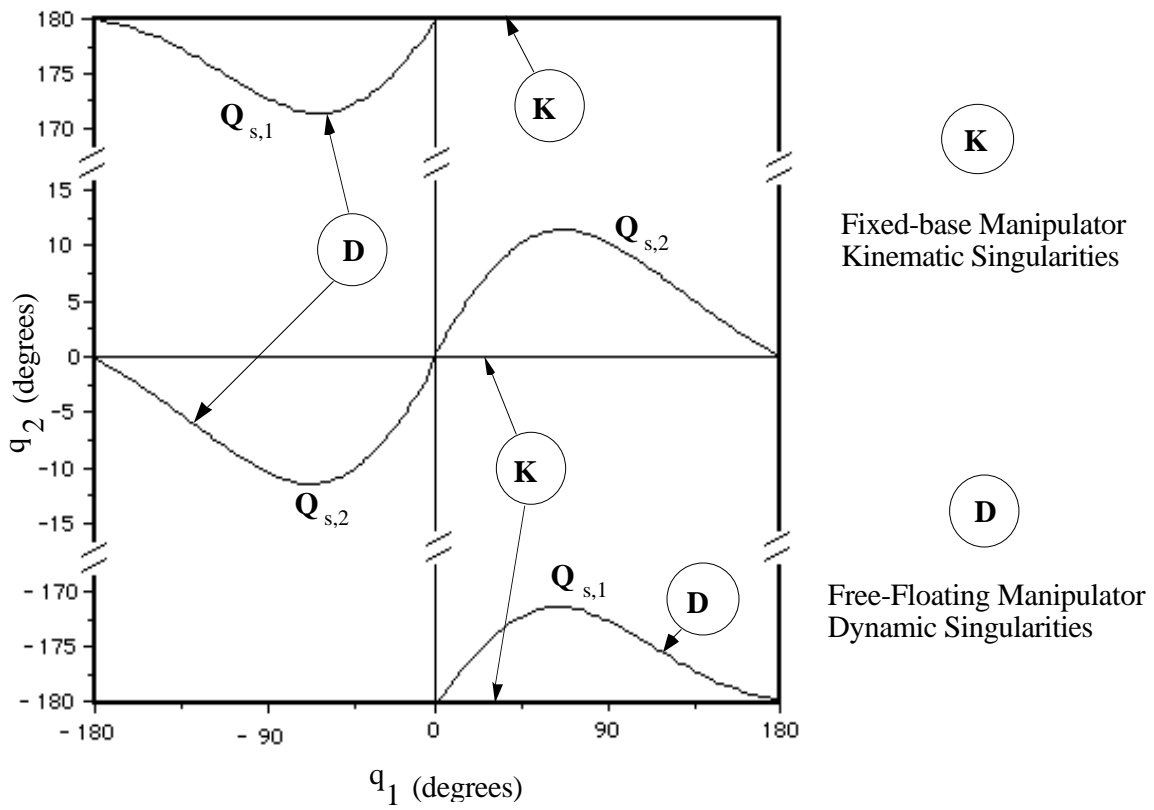Figure 3 A planar free-floating manipulator system shown in a dynamically singular configuration.

Figure 4. Dynamically singular configurations (q_1, q_2) for the two link manipulator in joint space.
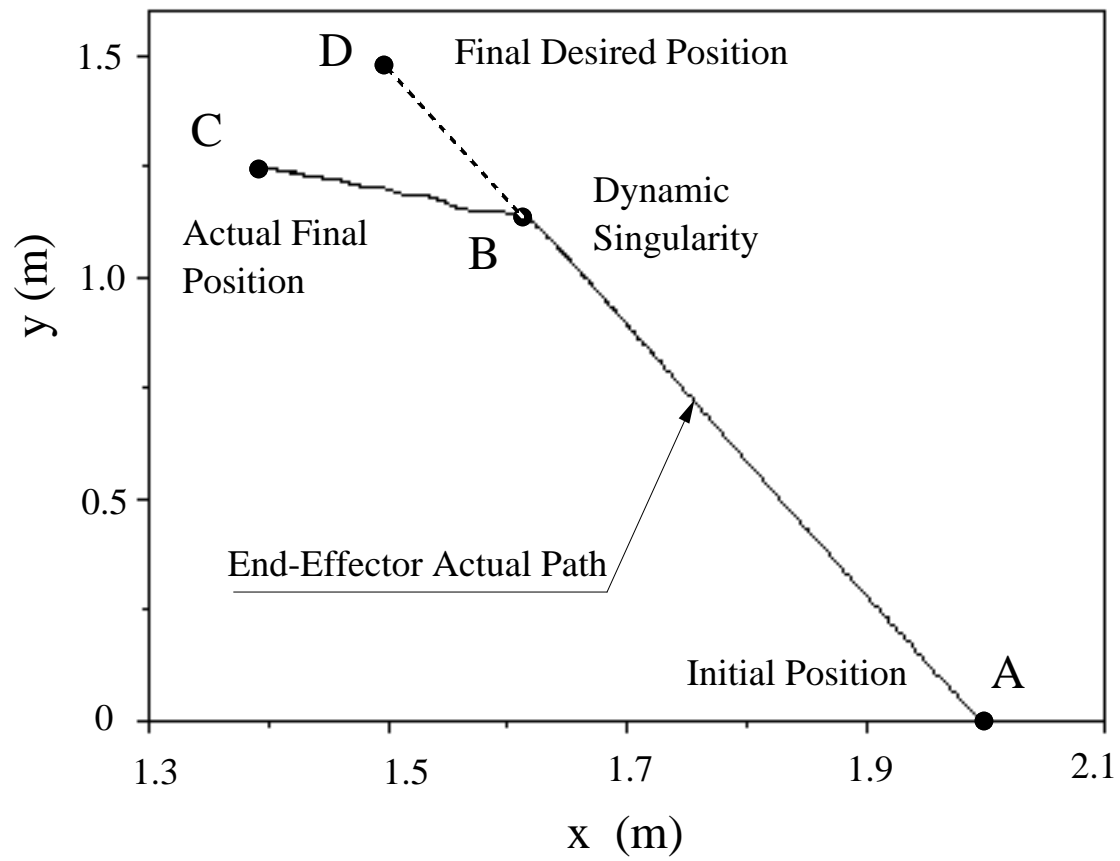
Figure 5.   Dynamic Singularities result in large tracking errors.
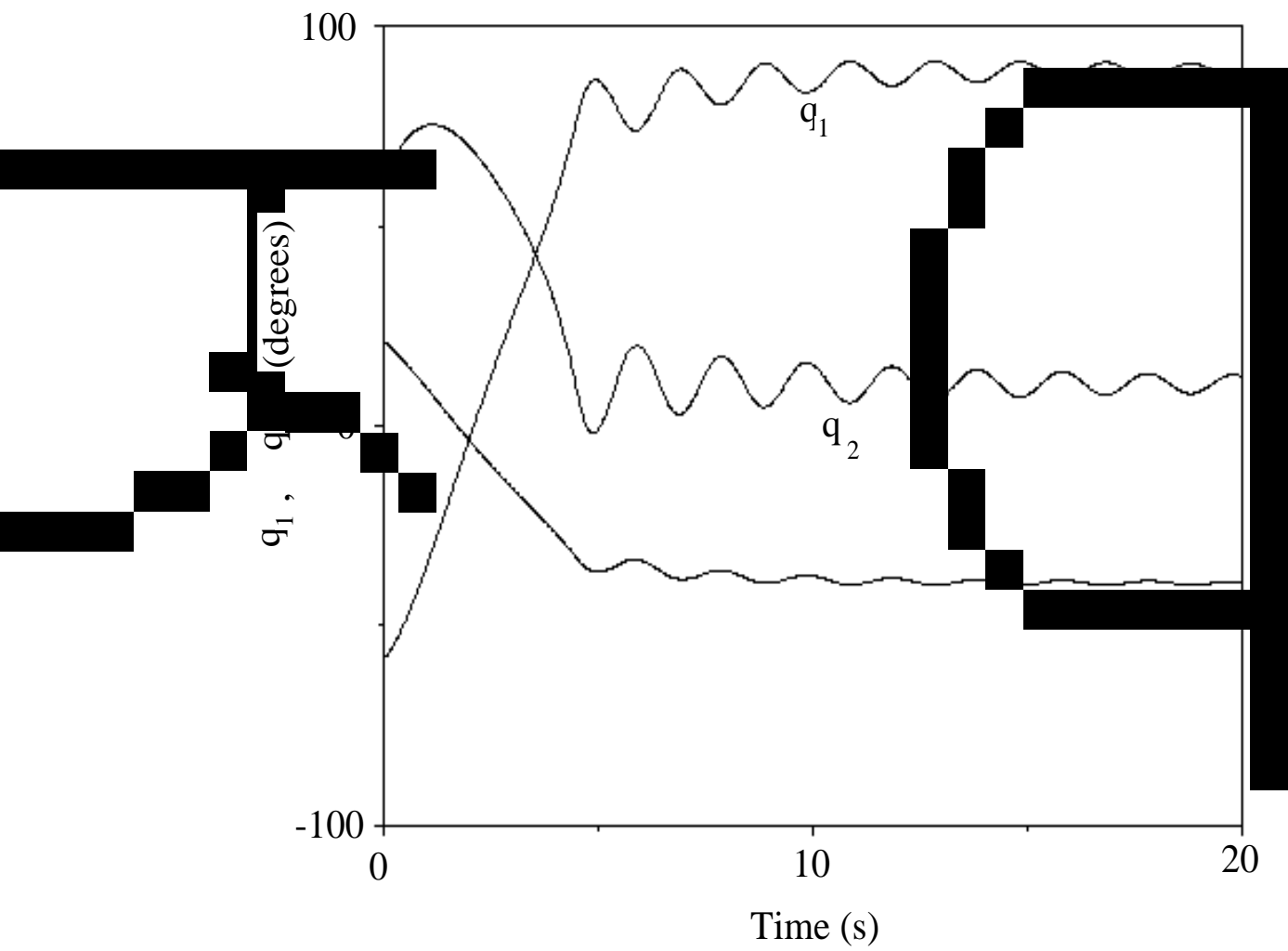
Figure 6. The spacecraft attitude θ and the manipulator joint angles q_1 and q_2 as a function of time.
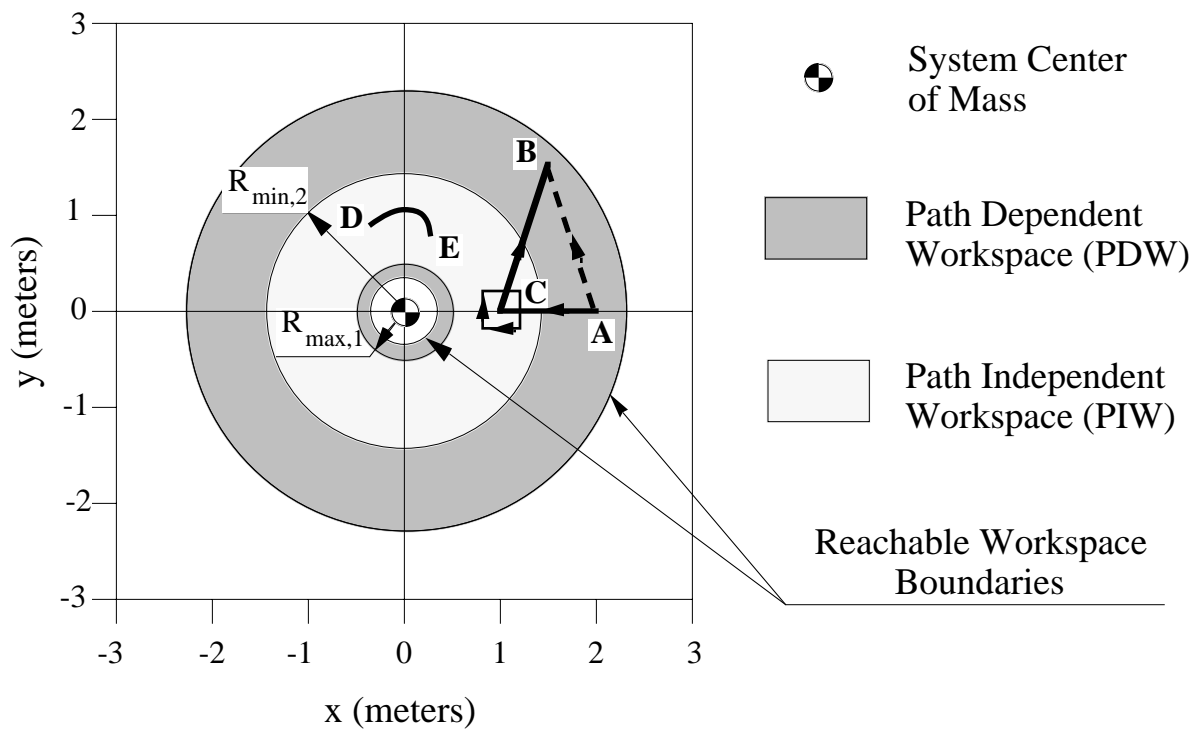
Figure 7.   The Reachable, the Path Dependent, and Path Independent Workspaces. Point B is
not reachable from point A following the straight line path AB, but it is reachable
following the path ACB.